Adaptive Modeling and Long-Range Prediction of Wireless Channel Fading

Abdorreza Heidari and Amir K. Khandani

Technical Report UW-E&CE #2006-04

Coding & Signal Transmission Laboratory

Department of Electrical & Computer Engineering

University of Waterloo

Waterloo, Ontario, Canada, N2L 3G1

January 2006

Adaptive Modeling and Long-Range Prediction of Wireless Channel Fading

Abdorreza Heidari and Amir K. Khandani

Coding and Signal Transmission Laboratory (www.cst.uwaterloo.ca)

Dept. of Elec. and Comp. Eng., University of Waterloo

Waterloo, ON, Canada, N2L 3G1

Tel: 519-883-3950, Fax: 519-888-4338

E-mails: {reza,khandani}@cst.uwaterloo.ca .

Abstract

Coherent communication requires that channel estimates be available at the receiver. These estimates are usually obtained using some sort of preamble or pilots. Powerful pilots may not be available in some systems as they consume a big part of the transmit power. Therefore, we propose a novel channel prediction algorithm that works well in the case that channel estimates are not accurate. Our simulations show that this algorithm is excellent for long-range prediction, which could be very helpful for other parts of the communication system as well.

Index Terms

Channel Modeling, Long-Range Prediction, Wireless/Mobile Channel Fading, State-Space Model, Kalman Filtering, Linear Prediction

I. Introduction

In this article, the issue of channel fading modeling and prediction is addressed. Channel fading prediction can be used to improve the performance of telecommunication systems including 3G systems. Having some estimates of future samples of the fading coefficients facilitates and enhances the performance of many tasks of the receiver or the transmitter, such as channel equalization, the decoding process of data symbols, antenna beamforming, and adaptive modulation schemes. In this article, a novel channel model is utilized for prediction of channel fading. This model is used in a Kalman filter to introduce a powerful fading prediction algorithm. The Simulation chapter demonstrates the effectiveness of this approach.

The rest of this report is organized as follows. Jakes fading and a general fading model are explained. Then, the existing approach on the channel evolution models is surveyed, a new model is introduced. Section IV includes the simulation results where our fading prediction algorithm is compared to the popular linear prediction algorithm.

II. Involved Models

A. System Model

Consider a system with two transmit antennas and one receive antenna. As a channel model, a flat fading channel [1] is considered from each transmit antenna to the receive antenna. At time instance n, we write

$$r_n = \underline{\mathbf{h}}_n^T \underline{\mathbf{x}}_n + n_n, \tag{1}$$

where r_n is the received signal at the receiver,

$$\underline{\mathbf{h}}_n = [h_n^{(1)}\ ,\ h_n^{(2)}]^T \in \mathbb{C}^2 \tag{2}$$

is our channel coefficients complex vector, where $h_n^{(m)}$ represents the channel between the m-th transmit antenna and the receive antenna,

$$\underline{\mathbf{x}}_n = [x_n^{(1)}\ ,\ x_n^{(2)}]^T \in \mathbb{C}^2 \tag{3}$$

represents the channel input vector. n is a complex circularly symmetric AWGN with the variance N_0, $n \sim \mathcal{N}(0, N_0)$, which can model the noise and possibly some other interferences.

B. Jakes Fading Model

In wireless communication systems, the received signal experiences significant power fluctuations due to fading. Signal fading is caused by multipath propagation and Doppler frequency shift. Multiple scatterers causes interference between reflected transmitter signal components. As the mobile drives through this interference pattern, it experiences a specific fading pattern which is unique for the mobile path and the scattering environment and is usually time-varying.

The superposition of component waves leads to either constructive or destructive interference, which make the fading peaks and deep fades, respectively. When all delayed components arrive at the receiver within a small fraction of the symbol duration, the fading channel is frequency-nonselective, or flat. This often occurs in narrowband signaling. Consider an environment with no dominant line-of-sight between the transmitter and the receiver. It is well-known that the envelope of a transmitted carrier at the receiver has the Rayleigh distribution, whereas the phase is uniform [1].

Assuming a two-dimensional *isotropic* scattering and an omni-directional receiving antenna, it is known that power spectral density (PSD) of the fading process is given by

[2]

$$S_h(f) = \begin{cases} \frac{1}{\pi f_d} \frac{1}{\sqrt{1-\left(\frac{f}{f_d}\right)^2}}. & |f| < f_d \\ 0, & \text{otherwise}, \end{cases} \tag{4}$$

where f_d is the maximum doppler frequency. Alternatively, the autocorrelation function of the process is shown as [2]

$$R_h(t, t-\tau) = \frac{E[h(t)h^*(t-\tau)]}{\sigma_h^2} = J_0(2\pi f_d \tau), \tag{5}$$

where $J_0(\cdot)$ is the first-kind Bessel function of the zero order and τ is the time difference. The Jakes model, also known as Clarke's model, is a special case of the general fading model explained in the next section, and is mathematically valid for a rich-scattering environment, i.e., when the number of the scatterers is significant.

The Jakes fading generator [2] has been used for several decades to simulate mobile channels. Based on the original model, some new models have been proposed to improve the properties of the generated fading signal. In [3], an improved model is suggested which generates a wide-sense stationary (WSS) signal, unlike the original Jakes model which is deterministic. The previous report [4] elaborates on the improved Jakes model which is used in our simulations.

C. A General Fading Model

Jakes fading is resulted from a statistic modeling of fading. However, fading could be observed as a deterministic signal. When the receiver, the transmitter, and/or the scatterers are moving, each scattered component undergoes a Doppler frequency shift given approximately by [5], [6]

$$f_k = f_d \, cos(\theta_k) \tag{6}$$

where θ_k is the incident radiowave angle of the k'th component with respect to the motion of the mobile and f_d is the maximum doppler frequency defined as

$$f_d = \frac{v}{c} f_c \tag{7}$$

where f_c is the carrier frequency, v is the mobile speed and c is the light speed. Assuming N_{sc} scatterers, the complex envelop of the flat fading signal at the receiver is

$$h(t) = \sum_{k=1}^{N_{sc}} a_k \, e^{j(\omega_k \, t + \phi_k)} \tag{8}$$

where for the n'th scatterer, a_k is the (real) amplitude, ϕ_k is the initial phase, and $\omega_k = 2\pi f_k$ where f_k is defined in (6). In real mobile environments, usually there are a few main scatterers which construct the fading signal [7].

We assume flat fading for the channel here, i.e., one resolved multipath component. But the same analysis could apply to each resolved multipath component in case the delays were not negligible in comparison to the symbol period [8].

D. Estimation of the General Fading Parameters

Assuming N_{sc} scatterers, there are $2\,N_{sc}$ unknown parameters to be determined for the model. Using $2\,N_{sc}$ fading samples, an equation set could be solved to find ω_k and $\alpha_k, k = 1, \ldots, N_{sc}$ (For details, refer to [4]). But it is evident that using noisy measurements could result in poor estimations. Let's look at the problem in the frequency domain.

Fourier transform of the fading signal shown in (8) is

$$H(\omega) = \sum_{k=1}^{N_{sc}} \alpha_k \, \delta(\omega - \omega_k) \tag{9}$$

Therefore the components are decoupled in the frequency domain and it is appropriate to find the parameters using Fourier transform, which can be implemented using FFT [9] over the observation window. This analysis gives a very good estimation of ω_k's if

the doppler frequencies does not change drastically over the window (This may happen if the mobile does an abrupt path change). ω_k's are usually changing slowly. Therefore, we will be using an adaptive algorithm to to track the doppler frequencies.

As it can be seen in (9), α_k's also may be estimated from the fourier analysis. But α_k's usually change faster than ω_k's as mobile moves and the scattering environment changes. Therefore, knowing ω_k's, we will apply Kalman filter to efficiently track α_k's.

The next section explains the existing channel evolution models. Then we will introduce an state-space model of the general fading formulation, which is utilized in a Kalman filter later.

E. Channel Evolution Model

To predict a process, a time evolution model of the process is required. A linear model, i.e. an auto-regressive moving-average (ARMA) model, is easy to use. But the fading process represented in (4) (or equivalently in (5)) is highly nonlinear, and can not exactly be modeled with a reasonable linear filter. Therefore, an approximate low-order AR model is widely used which can capture most of the fading dynamics [10], [11]. From now on, we consider one fading channel from one transmit antenna to a receive antenna, because we assume that the channels are uncorrelated and undergo the same condition (e.g. the same doppler frequency). Moreover, we consider a single path fading for simplicity, because the same model could be used for each fading path.

1) Linear Models: Assuming a first-order AR model, shown as AR(1), for the fading coefficient, the evolution equation is

$$h_n = a_1 \, h_{n-1} + g_0 \, q_n \tag{10}$$

where a_1 is the AR coefficient, and q_n is a complex white Gaussian noise process with the variance σ_h^2. For stability, $|a_1| \leq 1$. The gain of the noise process is $g_0 = \sqrt{1 - |a_1|^2}$

to keep the power of the process constant. From (5) and (10), it can be simply shown that $a_1 = J_0(2\pi f_d\, T)$, where T is the time distance between the channel samples. This value of AR coefficient matches the first correlation coefficient of the AR process with the original fading process.

For carrier frequency of f_c, we have $f_d = \frac{f_c}{3\times 10^8}\, v$, where v is the mobile speed. Assuming that the channel fading is sampled each $T = 1/1500$ second and $f_c = 2$ GHz, we have $f_d\, T = .0012\, v$, where v is the mobile speed (in kmph). Hence, for $v < 100$ kmph, $f_d\, T < .12$ which means $a_1 > .86$.

The AR(1) estimation model can be extended to an AR(p) model, which follows

$$h_n = a_1\, h_{n-1} + a_2\, h_{n-2} + \cdots + a_p\, h_{n-p} + g_0\, q_n. \tag{11}$$

2) State-Space Representation: An evolution model can be shown as a state-space model, as follows:

$$\begin{cases} \mathbf{x}_n = \mathbf{A}_n\, \mathbf{x}_{n-1} + \mathbf{q}_n \\ \\ z_n = \mathbf{M}_n\, \mathbf{x}_n + v_n \end{cases} \tag{12}$$

where $\mathbf{x}_n$ is a $N \times 1$ state vector at time n, $\mathbf{A}_n$ is a $N \times N$ matrix which controls the transition of the state vector in time, and $\mathbf{q}_n$ is a (usually Gaussian) noise vector, with the covariance of $\mathbf{Q} = E[\mathbf{q}_n\, \mathbf{q}_n^H]$, which represents the model error. Also $\mathbf{M}_n$ is known as the measurement matrix, and v_n is the observation noise with the variance σ_v^2. In effect, z_n is the system output which is the available (noisy) measurement of the state. In practical systems of interest, $\mathbf{A}_n$, $\mathbf{Q}$ and $\mathbf{M}_n$ are usually constant or very slow time-varying.

Note that the state-space representation of a specific system is usually not unique. A well-known state-space representation of the linear model of (11) can be found in [4].

3) Our State-Space Model:: For the general fading model, we propose the following state-space model

$$\mathbf{A}_n = diag\left[e^{j\omega(1)\,Ts},\, e^{j\omega(2)\,Ts},\, \ldots,\, e^{j\omega(N)\,Ts}\right] \tag{13}$$

and

$$\mathbf{M}_n = [1,\, 1,\, \ldots,\, 1] \tag{14}$$

where $z_n = \hat{h}_n$ is the available channel estimate, and

$$\mathbf{x}_n = \left[\alpha(1)\, e^{j\, n\omega(1)\,Ts},\, \alpha(2)\, e^{j\, n\omega(2)\,Ts},\, \ldots,\, \alpha(N)\, e^{j\, n\omega(N)\,Ts}\right]^T \tag{15}$$

III. Prediction

A. Linear Prediction

A linear predictor of order p, with the prediction depth of D is shown as follows

$$\begin{aligned} \hat{h}_n &= a_D\, h_{n-D} + \cdots + a_{D+p-1}\, h_{n-D-p+1} && (16)\\ &= \sum_{i=0}^{p-1} a_{D+i}\, h_{n-D-i}. && (17) \end{aligned}$$

Minimizing the mean square error (MSE) provides the required coefficients, i.e.,

$$\begin{aligned} &\min E\left[\left|h_n - \hat{h}_n\right|^2\right] = \\ &\min_{a_D,\ldots,a_{D+p-1}} E\left[\left|h_n - \left(\sum_{i=0}^{p-1} a_{D+i}\, \overline{h}_{n-D-i}\right)\right|^2\right], \end{aligned} \tag{18}$$

where $\overline{h}_n = h_n + v_n$ is the noisy estimate of the channel fading. The observation SNR is defined as $\mathrm{SNR}_z = \sigma_h^2/\sigma_v^2$ which is assumed to be known. Also we assume $\sigma_h^2 = 1$.

It is well-known that the solution of (18) can be found by solving the Yule-Walker equations [12], which is

$$\mathbf{a} = \mathbf{R}^{-1}\,\mathbf{R_0} \tag{19}$$

where $\mathbf{a}, \mathbf{R}$ and $\mathbf{R_0}$ are defined as follows. $\mathbf{a} = [a_D\, a_{D+1}\, \cdots\, a_{D+p-1}]^T$ is the coefficient vector, $\mathbf{R} = [R_{ji}]_{p\times p}$ is the data correlation matrix where

$$R_{ji} = E[\overline{h}_{n-D-i+1}\, \overline{h}^*_{n-D-j+1}] \tag{20}$$

$$= \sigma_h^2\, J_0(2\pi f_d T\ |j-i|) + \sigma_v^2\, \delta(j-i), \tag{21}$$

where

$$\delta(k) = \begin{cases} 1, & k = 0 \\ 0, & k \neq 0 \end{cases} \tag{22}$$

and $\mathbf{R0} = [R_{0j}]_{p\times 1}$ where

$$R_{0j} = E[h_n\, \overline{h}^*_{n-D-j+1}] \tag{23}$$

$$= \sigma_h^2\, J_0(2\pi f_d T\ |j+D-1|) + \sigma_v^2\, \delta(D+j-1). \tag{24}$$

The corresponding mean square error defined in (18) is

$$\mathrm{MSE}_{\mathrm{out}} = \sigma_h^2 - \sum_{j=1}^{p} a_{D+j-1}\, R_{0j}. \tag{25}$$

Note that the input samples to the linear predictor has the MSE of $\sigma_v^2 = 1/\mathrm{SNR}_z$, while the output estimate error is $\mathrm{MSE}_{\mathrm{out}}$ defined as above.

In practice, channel coefficients are estimated (using the common pilots,...) which usually introduces some error in the available channel coefficients. Here, the channel estimation error is modelled as an Additive White Gaussian Noise (AWGN), and Observation SNR, SNR_z, is defined as the ratio of the channel power to the noise power. Fig. 1 demonstrates the MSE of the linear prediction versus mobile speed for different linear orders at different SNR_z. It is observed that at each SNR_z and each mobile speed, there is an optimum order p which could be different at other situations. This variable order makes the implementation of the prediction algorithm difficult. Therefore, for the SNR_z corresponding to a specific application, an overall-good order should be chosen.

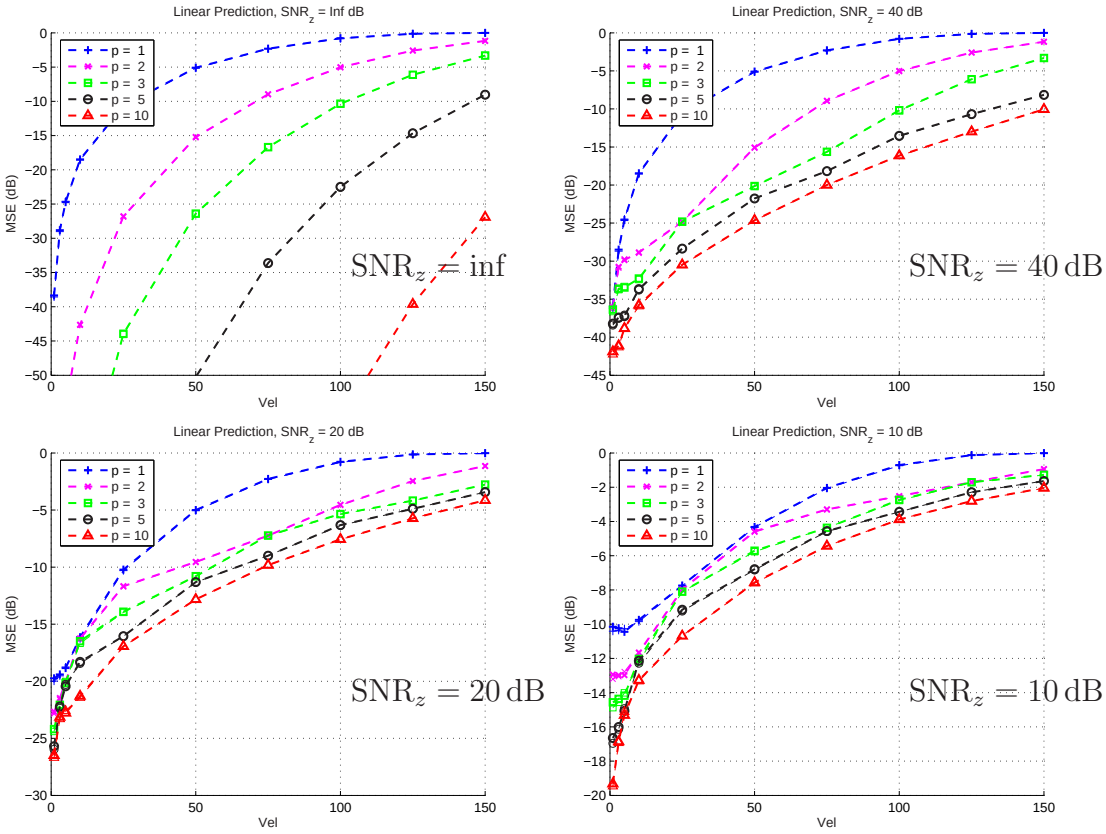

Fig. 1. Linear Prediction MSE versus mobile speed in different observation SNR's for Jakes fading

For example, consider $\mathrm{SNR}_z = 40\,dB$. For low to moderate mobile speeds, $p = 2$ is optimum, while at high mobile speed, $p = 3$ or 4 seem better.

B. Kalman Filtering

Kalman Filtering is now commonly used in communication systems (for example, see [13]). Assuming a state-space model, Kalman filter efficiently estimates the state vector $\mathbf{x}_n$ which will be used to predict the future samples of the fading signal.

Table I defines the variables used in the Kalman equations, which follow:

Prediction part:

$$\mathbf{x}_n^- = \mathbf{A}\,\mathbf{x}_{n-1}^+ \tag{26}$$

$\mathbf{Q}$	The covariance matrix of the model noise
z_n	The observation sample
$\mathbf{x}_n^-$	The *a priori* estimate of the state $\mathbf{x}_n$ (sometimes shown as $\mathbf{x}_{n\|n-1}$)
$\mathbf{x}_n^+$	The *a posteriori* estimate of the state $\mathbf{x}_n$, i.e., with having the observation z_n (sometimes shown as $\mathbf{x}_{n\|n}$)
$\mathbf{P}_n^-$	The covariance matrix of the *a priori* error
$\mathbf{P}_n^+$	The covariance matrix of the *a posteriori* error

TABLE I

VARIABLES USED IN KALMAN FILTER

$$\mathbf{P}_n^- = \mathbf{A}\,\mathbf{P}_{n-1}^+\mathbf{A}^T + \mathbf{Q} \tag{27}$$

Update part:

$$\mathbf{x}_n^+ = \mathbf{x}_n^- + \mathbf{K}_n\left(z_n - \mathbf{M}_n\,\mathbf{x}_n^-\right) \tag{28}$$

$$\mathbf{P}_n^+ = \Big(\mathbf{I} - \mathbf{K}_n\,\mathbf{M}_n\Big)\mathbf{P}_n^- \tag{29}$$

where

$$\mathbf{K}_n = \mathbf{P}_n^-\,\mathbf{M}_n^H\left(\mathbf{M}_n\,\mathbf{P}_n^-\,\mathbf{M}_n^H + \sigma_v^2\right)^{-1}. \tag{30}$$

Assuming the current state $\mathbf{x}_n$, which carries all the information about the past, future channel state should be predicted. It has been shown in [14] that the MMSE estimate of the D-step prediction is

$$\hat{\mathbf{x}}_{n+D} = \mathbf{A}^D\,\mathbf{x}_n. \tag{31}$$

Hence, the predicted channel coefficient is $\hat{h}_{n+D} = \mathbf{M}\,\hat{\mathbf{x}}_{n+D}$.

IV. SIMULATION

A. The Fading Prediction Algorithm

It was observed in the previous section that fading prediction can result in significant savings in transmit power. Linear prediction is used at the mobile unit, which is good enough for some applications. But the performance of a linear predictor may not be enough, for example, for low observation SNR's. The linear approach has a poor performance at high mobile speeds as well, as it is solely dependent on the correlation parameters of the fading process.

We propose a fading prediction algorithm here for improving the prediction at low observations SNR's, and high mobile speeds. Fig. (2) shows the flowchart of the prediction algorithm. A description of the main blocks follows. Kalman filtering and the prediction part are explained in Section III-B.

1) Doppler Frequencies: The required parameters for the fading are estimated according to Section (II-D). Assume N_{sc} as the number for the scatterers.

2) Acquisition:: We apply the Fourier method explained in Section (II-D) to estimate the $\omega(k), k = 1, \ldots, N_{sc}$ by performing FFT over an observation window of N_{win} recent samples, $H = FFT[h]$. We have used an FFT length of $N_{FFT} = 2\,N_{win}$, to increase the frequency resolution. Therefore, each sinusoid can be projected upto 3 samples in H. Therefore, first the peak of H is found, and then the $\omega(1)$ is calculated by averaging over the amplitudes of the three adjacent frequency samples. An initial estimate of $\alpha(1)$ is also achieved in this way. Other $\omega(k)$ and $\alpha(k)$'s are found by continuing this procedure.

Acquisition could be done frequently to keep the frequency doppler estimates updated. However, to decrease the required computations, it could be done only if the error trend passes a threshold. Also the algorithm does not allow two consecutive acquisitions

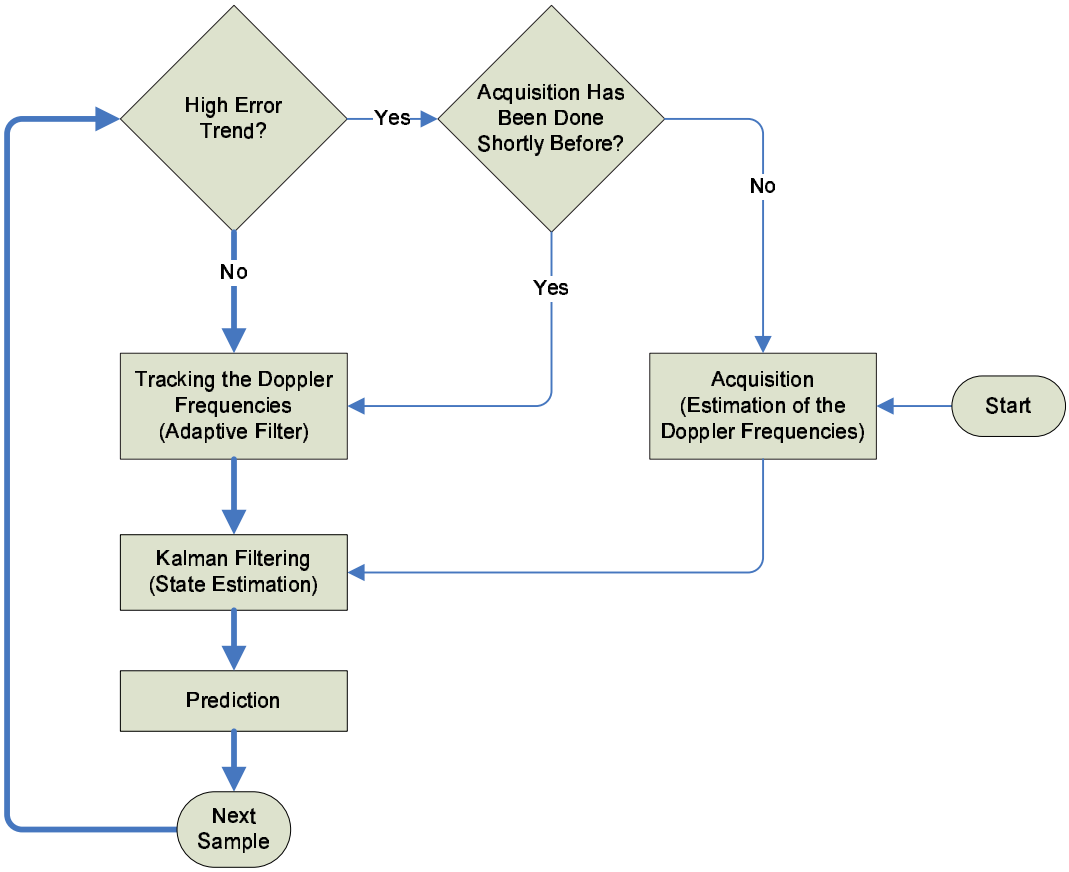

Fig. 2. Block Diagram of our Prediction Algorithm (KF)

to be too close. Because after each acquisition, other blocks of the algorithm should have enough time to catch up with the new frequency estimates.

3) Tracking: An adaptive algorithm is used to track the fine changes of the doppler frequencies. Using a gradient-based approximate, the following LMS algorithm can be applied

$$w_{n+1}(k) = w_n(k) + \mu\, \mathbf{X}_n^+(k)^H\, \mathbf{M}_n(k)^H\, e_n, \tag{32}$$

where

$$e_n = z_n - \hat{h}_n, \tag{33}$$

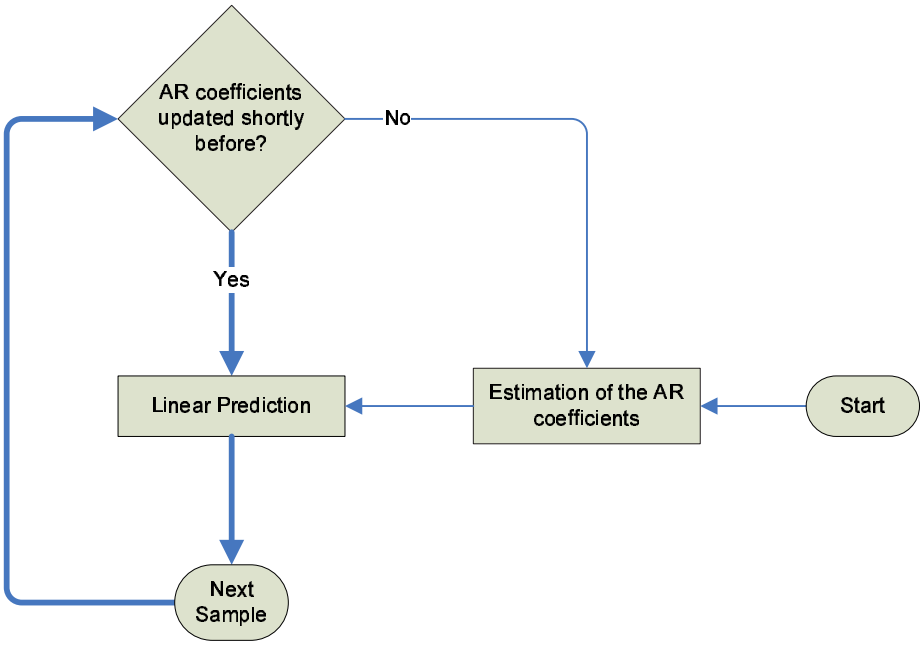

Fig. 3. Block Diagram of the Linear Prediction Algorithm (LP)

where

$$\hat{h}_n = \mathbf{M}_n \, \mathbf{X}_n^{+}. \tag{34}$$

4) Calculation of the Error Trend: We use an exponential window for calculation of the error trend from sample errors, as follows

$$E_{n+1} = \lambda_E \, E_n + (1 - \lambda_E) \, |e_n|^2 \,, \tag{35}$$

where λ_E is the forgetting factor ($0 \ll \lambda_E < 1$).

5) The Linear Prediction Algorithm: The block diagram of the linear prediction algorithm is shown in Fig. 3. Estimation of the AR coefficients is done frequently, by using the `lpc(·)` function of MATLAB. As opposed to our algorithm, here we do not decrease the computational complexity by looking at the error trend, because we want to get the best achievable performance out of the linear prediction.

6) Simulation Results: The two prediction algorithms are compared here (LP and KF), with respect to the average MSE versus the prediction depth, at $\mathrm{SNR}_z = 10$ dB.

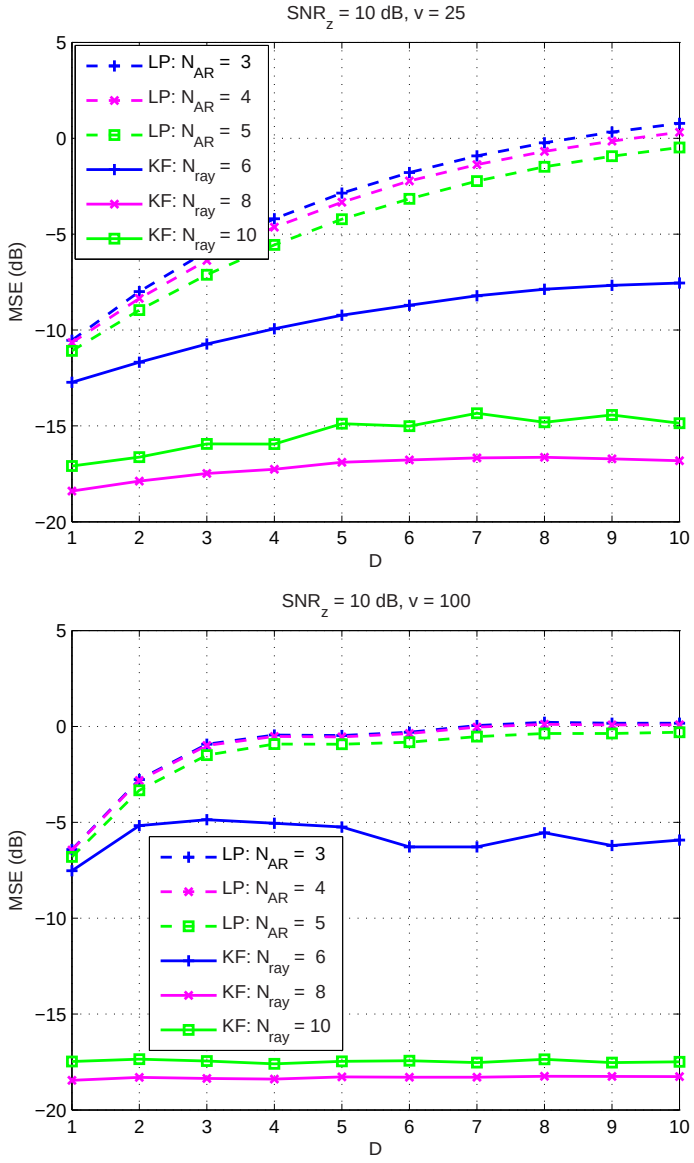

Fig. 4. Comparison of MSE versus prediction depth for Jakes fading at v=25 and v=100

The results are reported for various linear orders N_{AR}, and various scattering orders N_{ray}, respectively (N_{ray} is an estimate of N_{sc} in (8)). Fig. 4 show the results for Jakes fading for v=25 and v=100 kmph. It is observed that KF significantly outperforms LP if N_{ray} is large enough ($N_{\mathrm{ray}} \leq 8$), while LP fails at high prediction depths regardless of the linear order.

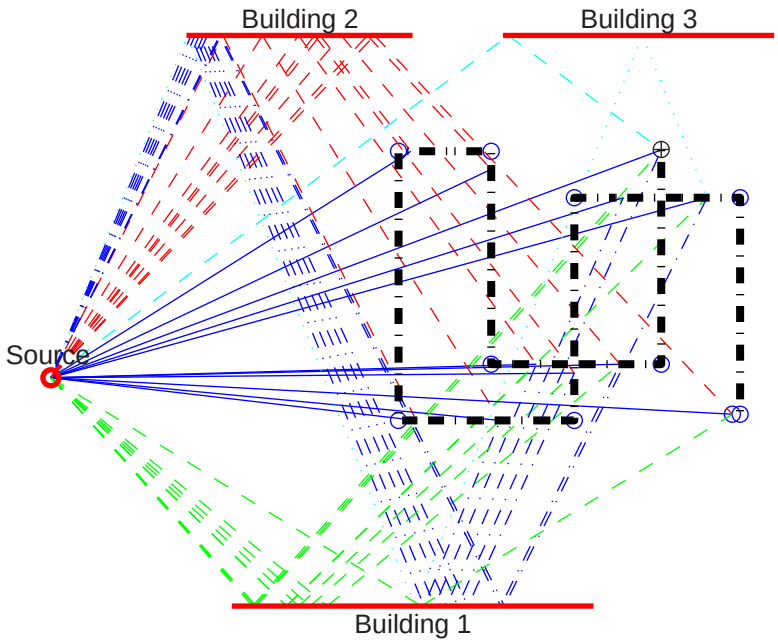

Fig. 5. A typical mobile environment for generation of RT fading

Jakes fading is valid for a rich scattering area. We want to test the algorithms with a more realistic fading signal. So we use the Ray-Tracing simulation environment explained in [4] to generate the “RT fading”. Fig. 5 shows the environment which was used to generate RT fading here. The mobile is randomly moving vertically and horizontally in the scattering area and experiences different combination of signal rays. At each point of the mobile path, it undergoes a different doppler frequency and a different signal power for each ray. Therefore, the generated fading can closely resemble the fading in a real mobile environment.

Fig. 6 show the results for a ray-tracing (RT) fading for v=25 and v=100 kmph. It is observed that always KF outperforms LP. As RT fading represents not a very rich scattering environment, it is observed that increasing N_{ray} does not necessarily improves the performance. Note that LP is sensitive to the linear order at high mobile speeds. In fact, it is observed in our simulations that a linear model is not dependable for higher mobile speeds because the pattern of the performance fluctuations follows the correlation

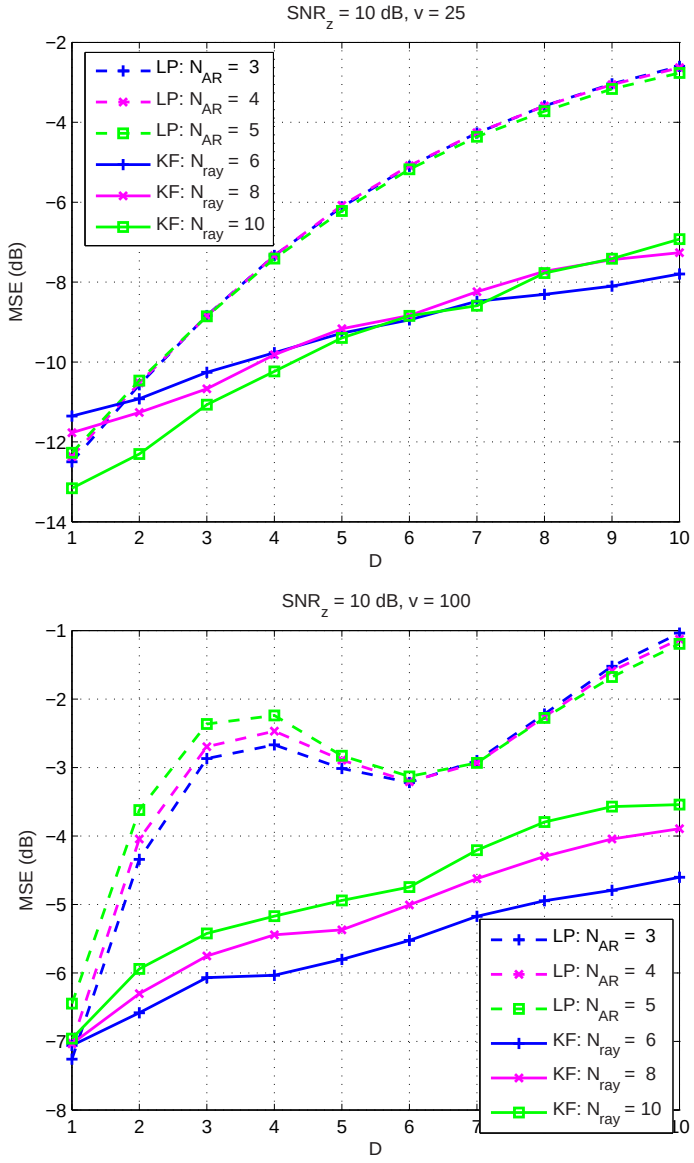

Fig. 6. Comparison of MSE versus prediction depth for RT fading at v=25 and v=100

properties of the fading, i.e., a lower correlation at a time difference results in a higher MSE for that prediction depth.

REFERENCES

[1] J. G. Proakis, *Digital Communications*. Mc-Graw Hill International Editions, 2001.

[2] W. C. Jakes, Ed., *Microwave Mobile Communications*. New York: IEEE Press, 1974.

[3] M. F. Pop and C. Beauliu, “Limitations of Sum-of-Sinusoids Fading Channel Simulators,” *IEEE Trans. on Communications*, Apr. 2001.

[4] A. Heidari, A. K. Khandani, and D. McAvoy, “Channel Prediction for 3G Communication Systems,” tech. rep., Bell Mobility, Aug. 2004.

[5] T. S. Rappaport, *Wireless Communications: Principles and Practice*. Prentice-Hall, 1996.

[6] A. Duel-Hallen, S. Hu, H. Hallen, “Long Range Prediction of Fading Signals: Enabling Adaptive Transmission for Mobile Radio Channels,” *IEEE Signal Processing Magazine*, May 2000.

[7] T. Eyceoz, A. Duel-Hallen, and H. Hallen, “Deterministic Channel Modeling and Long Range Prediction of Fast Fading Mobile Radio Channels,” *IEEE Communications Letters*, Sept. 1998.

[8] H. Hallen, S. Hu, A. Duel-Hallen, “Physical Models for Understanding and Testing Long Range Prediction of Multipath Fading in Wireless Communications,” *submitted to IEEE Transactions on Vehicular Technology*.

[9] A. V. Oppenheim, R. W. Schafer, and J. R. Buck, *Discrete-Time Signal Processing*. Prentice Hall, 1999.

[10] C. Komninakis, C. Fragouli, A. H. Sayed, and R. D. Wesel, “Muti-Input Multi-Output Fading Channel Tracking and Equalization Using Kalman Estimation,” *IEEE Trans. on Signal Processing*, May 2002.

[11] M. Yan and B. D. Rao, “Performance of an Array Receiver with a Kalman Channel Predictor for Fast Rayleigh Flat Fading Environments,” *IEEE Journal on selected Areas in Communications*, 2001.

[12] A. Papulis, *Probability, Random Variables, and Stochastic Processes*. McGraw-Hill, 1984.

[13] H. Gerlach et al., “Joint Kalman Channel Estimation and Equalization for the UMTS FDD Downlink,” *IEEE 58th Vehicular Technology Conference (VTC’Fall)*, pp. 1263–1267, Oct. 2003.

[14] G. Janacek and L. Swift, *Time Series: Forecasting, Simulation, Applications*. Prentice Hall, 1993.